29. THE DOWNHOLE VARIATION OF THE ROCK-MAGNETIC PROPERTIES OF LEG 73 SEDIMENTS[1]

Peter Tucker,[2] Department of Geophysics, University of Edinburgh, Mayfield Road, Edinburgh, United Kingdom
and
Lisa Tauxe,[3] Lamont-Doherty Geological Observatory, Palisades, New York

ABSTRACT

The magnetic stability and mean intensity of the natural remanent magnetization (NRM) of Leg 73 sediments (Holes 519 to 523) decreases with the age of the sediment. We demonstrate that these variations are linked with physical and chemical changes in the magnetic grains themselves. Alteration of the magnetic component occurs most rapidly shortly after deposition. A significant magnetic alteration over the topmost few meters of the sediments is thought to be the result of oxidation. The modification of the NRM characteristics through the partial dissolution of the carbonate is largely accounted for by the effects of concentraion of the magnetic minerals. We apply the techniques of rock-magnetism and X-ray fluorescence analysis to clarify the physical and chemical mechanisms that affect the magnetic character of the sediment.

INTRODUCTION

The interpretation of the magnetic record carried by unconsolidated sediments relies heavily on the investigator's ability to deconvolute the part of the recording that is contemporaneous with the sediment formation. The primary magnetization is acquired through the physical alignment of the magnetic grains in the Earth's magnetic field. Physical processes can subsequently modify this alignment (Verosub, 1977; Tucker, 1980a and b). Indeed, many features of the sedimentary record can be readily explained in terms of a postdepositional realignment of the magnetic grains (Tucker, this vol.). However successful the physical theories may appear, however, they do not tell the whole story. Chemical alteration of the magnetic fraction can severely perturb or, in some cases, completely overprint the original recording (Kent and Lowrie, 1974; Henshaw and Merrill, 1980). In the present investigation, the paleomagnetic results yielded by the Miocene red clays were not always reliable (Tauxe et al., this vol.), a problem often encountered with partially dissolved pelagic sediments. Chemical overprinting has long been known to be a major cause of this behavior. Tucker (this vol.) has shown that physical disturbance may also accompany the dissolution event and cause a further deterioration in the magnetic signal. In the present study, significant proportions of magnetic phases not seen in the carbonate-rich sediments were found in the red clays. These phases were able to carry both stable and unstable magnetic overprints. At the time of writing they could not be definitely identified, and indeed their origin, whether by diagenesis or merely through concentration, was uncertain (Tucker, this vol.).

In many deep-sea sedimentary cores the paleomagnetic record deteriorates with depth (Opdyke et al., 1966; Kent and Lowrie, 1974; Johnson et al., 1975). This feature was also noted with the Leg 73 material (Tauxe et al., this vol.). Kent and Lowrie (1974) and Johnson et al. (1975) attribute the loss of resolution to progressive low-temperature oxidation (maghemitization) of the detrital magnetite, or titanomagnetite, grains. Haggerty (1970) correlated an increase in the concentration of manganese micronodules with the loss of clarity of the magnetic record. Powell and Ballard (1968) and Crecelius et al. (1973) showed that some of the nonmanganese compounds in these nodules were magnetic and capable of carrying a remanent magnetization. Henshaw and Merrill (1980) argue that authigenic Fe–Mn oxides and hydroxides are most likely to be the main carriers of chemical remanent magnetization (CRM) in pelagic sediments, particularly authigenic red clays. They further argue that although maghemitization does exist, its effects are of secondary importance. It must also be remembered that hematite and goethite, although weakly magnetic, are also potential carriers of CRM. Finally, physical disturbance during the initial stages of consolidation of the sediment may contribute to the deterioration of the magnetic record.

This paper examines the downhole variation of the magnetic mineralogy of Leg 73 sediments in order to help elucidate the factors (chemical and physical) that affect the clarity of the inferred magnetostratigraphy.

SAMPLING CONSIDERATIONS

Previous investigations of the magnetic changes in deep-sea sediments (e.g., Kent and Lowrie, 1974; Henshaw and Merrill, 1980) have concentrated on near-surface sediments deposited within the last few million years. These investigations have shown that a significant change in the measured magnetic properties sometimes occurs a short distance below the sediment/water interface. Similarly, alteration (i.e., oxidation) in uncovered deep-sea basalts usually occurs very rapidly after ex-

[1] Hsü, K. J., LaBrecque, J. L., et al., *Init. Repts. DSDP,* 73: Washington (U.S. Govt. Printing Office).

[2] Present address: Warren Spring Laboratory, Gunnels Wood Road, Stevenage, Hertfordshire, United Kingdom.

[3] Present address: Scripps Institution of Oceanography, La Jolla, California.

trusion and can reach an advanced state within less than a million years (Ryall and Hall, 1979). For both types of rocks it has been established that chemical interactions between the bottom waters and the individual magnetic grains are responsible for a large part of the observed alteration.

The present investigation includes a survey of near-surface sediments and extends the study to older sediments where the pore waters are essentially cut off from mixing with the circulating bottom water. Most of the data come from Site 519 (0 to 10 Ma), where the relatively high sedimentation rate afforded a high time/depth resolution. Samples were selected from those previously used for the magnetostratigraphic study. The sampling density was typically one per core (4.5 m), with higher densities over regions that showed a rapid change in lithology. The above samples were augmented with a small number taken at random from the upper sections of Holes 520, 521, 522, and 523. Further samples comprising one or two from selected lithologies were taken from the much older sediments from Holes 523 and 524.

Samples were selected mainly by color, and the initial results are presented as such. The colors referred to are merely gross indications of the sediment's lightness or darkness and rough divisions into reds, yellows, browns, and whites. More precise descriptions can be found in the Initial Core Descriptions for Leg 73. Specific lithologies have been analyzed in detail by Tucker (this vol.), and they will not be further discussed here.

BULK MAGNETIC HYSTERESIS PROPERTIES AS A FUNCTION OF LITHOLOGY

Induced Magnetization

The color of a sediment is a good indication of its calcium carbonate content. The lightest sediments are richest in carbonate, whereas the darker or more strongly colored are relatively deficient in carbonate (Fig. 1). The noncarbonate fraction, which includes the magnetic grains, fluctuates at levels between 5 and 40% at Site 519. An indication of the total amount of Fe-bearing minerals present within this fraction can be obtained from measurements of the saturation magnetization, M_s (the induced magnetization measured in high fields) and of the high-field susceptibility, χ_h (the slope of the hysteresis loop at high fields). M_s is a measure of the total of all magnetic material present, excluding the paramagnetic or superparamagnetic material. χ_h shows the contribution of the superparamagnetic and paramagnetic minerals and also the very-high-coercivity minerals (e.g., hematite) that are present. In the absence of these, χ_h will record the intrinsic diamagnetism of the sediment.

The magnetic hysteresis properties were measured by using a vibrating sample magnetometer. The measured values of M_s and χ_h, together with other hysteresis and stability parameters, are listed in Table 1. Typical hysteresis loops for the various colors of sediment are shown in Figure 2. Further examples contrasting the white and red sediments are given by Tucker (this vol.).

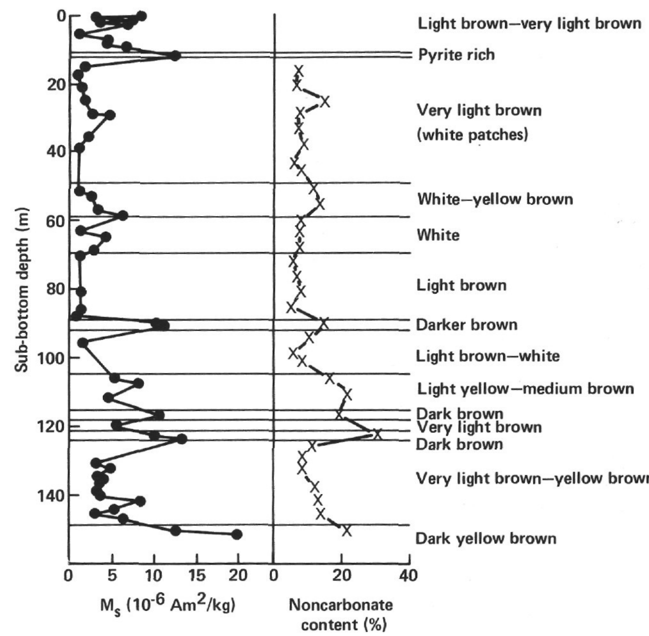

Figure 1. The correlation between the saturation magnetization (M_s), calcium carbonate content, and the color of the sediment. Hole 519.

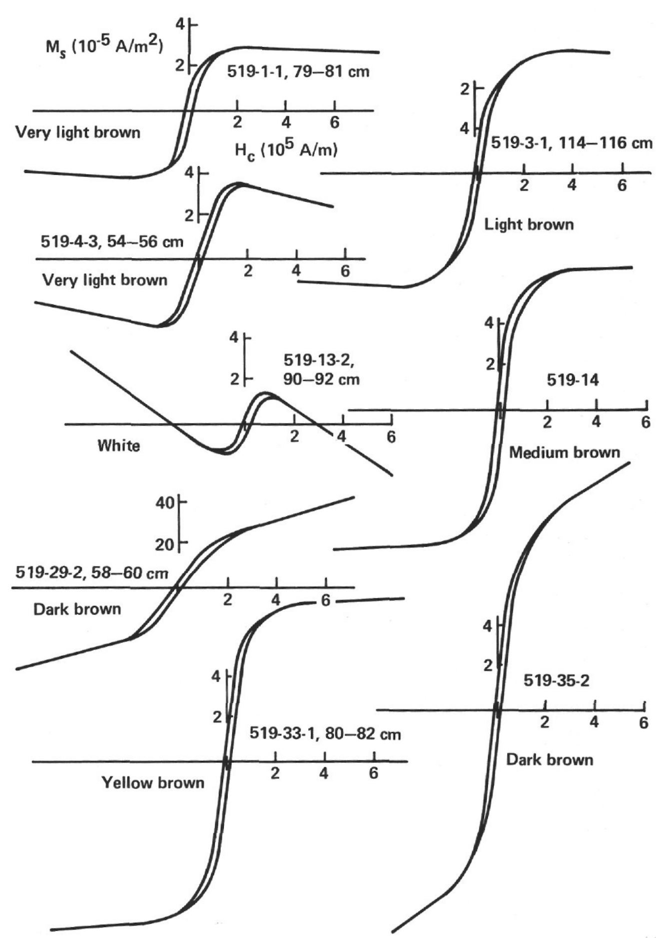

Figure 2. Magnetic hysteresis loops for sediment samples from Hole 519.

Table 1A. Downhole variation of the magnetic hysteresis and magnetic remanence parameters for Holes 519, 521, and 522.

Core-Section (interval in cm)	NRM (10^{-6} Am^2/kg)	M_{rs} (10^{-3} Am^2/kg)	χ_i (10^{-8})	χ_h (10^{-8} m^3/kg)	M_s (10^{-3} Am^2/kg)	H_c (10^4 A/m)	H_{cr} (10^4 A/m)	MDF (10^4 A/m)
Hole 519								
1-1, 19–21	13.04	2.16	4.98	5.03	8.42	1.55	3.85	—
1-1, 79–81	2.99	0.92	—	−1.43	3.43	1.47	—	—
1-1, 119–121	6.07	2.16	6.23	0.00	7.52	1.76	3.65	—
1-2, 24–26	2.39	1.27	—	0.00	3.75	1.46	—	—
1-2, 91–93	6.87	1.92	3.70	0.41	7.15	1.61	3.33	—
2-2, 69–71	1.30	0.52	0.82	−0.58	1.78	1.49	2.74	—
2-3, 79–81	9.08	1.41	2.90	0.00	4.36	1.79	3.54	
3-1, 114–116	2.07	1.63	5.86	0.00	5.00	1.37	2.86	—
3-2, 63–65	0.80	1.32	6.96	0.08	6.95	0.93	2.50	—
3-2, 138–140	2.78	1.42	—	0.34	6.55	1.44	2.94	—
3-3[a]	—	3.44	11.28	0.87	12.13	1.55	3.38	—
4-3, 54–56	0.68	0.63	1.77	−0.43	2.07	1.53	2.50	1.79
5-2, 86–88	0.41	0.48	1.26	−0.28	1.35	1.51	2.58	1.79
6-2, 90–92	0.60	0.48	3.67	−0.52	1.69	1.61	2.38	1.70
7-2, 91–93	0.46	0.40	1.54	−0.59	2.04	1.43	2.53	1.91
8-1, 80–82	0.96	0.61	2.28	0.69	2.71	1.41	2.42	2.03
8-2, 74–76	—	—	3.95	0.65	5.13	1.16	—	—
10-1, 52–54	—	0.72	2.51	−0.19	2.45	1.52	3.02	—
10-2	—	0.51	1.11	−0.54	1.95	1.52	2.54	1.79
13-2, 90–92	0.66	0.42	0.84	−1.00	1.38	1.61	2.54	—
13-3, 24–26	3.32	0.66	2.04	−0.65	2.90	1.49	3.06	—
14	—	0.82	3.88	0.04	3.85	1.09	2.46	—
15-1	—	1.32	7.35	1.76	6.70	1.09	2.07	—
16-1, 136–138	1.72	0.52	1.77	−0.51	1.82	1.71	3.02	1.74
16-2, 111–113	3.80	1.08	2.32	0.23	4.38	1.55	3.02	1.74
16-3, 130–132	0.26	0.46	1.42	—	—	1.26	2.58	1.56
17-2, 60–62	2.13	0.51	2.17	−0.76	2.59	1.44	2.58	1.71
17-2, 105–107	—	0.51	1.93	−0.75	1.64	1.26	—	—
20-2, 110–112	0.30	0.49	1.63	−0.82	1.62	1.34	2.46	—
21-1, 100–102	0.50	0.57	2.07	−0.46	1.83	1.31	2.46	—
21-1, 95–97	0.76	0.51	1.02	−0.69	1.75	1.31	2.26	1.63
21-3, 6–8	0.43	0.97	2.46	0.76	1.42	1.20	2.34	—
22-1	—	2.15	8.25	3.48	10.06	1.12	2.15	1.47
22-2	—	2.71	10.38	4.21	11.57	1.14	2.30	1.51
23-3, 38–40	0.51	0.57	2.01	−0.38	1.44	1.59	2.30	1.47
26-1	—	1.50	5.71	2.41	5.94	1.12	2.26	1.63
26-2	—	1.89	7.49	1.59	8.21	1.20	2.54	1.51
27	—	1.10	4.17	0.52	4.35	1.16	2.31	1.51
28-2, 14–16	—	2.38	9.40	7.65	11.08	1.12	2.15	1.51
29-1, 87–89	—	1.33	4.98	0.78	5.72	1.20	2.26	1.55
29-2, 58–60	1.29	2.41	9.96	3.78	10.00	1.09	2.18	1.59
29-3, 10–12	2.98	3.81	10.34	2.64	13.70	0.98	2.14	1.47
31-3, 94–96	1.50	0.89	3.54	−0.20	3.75	1.21	2.42	—
32-1, 97–99	0.46	0.95	3.81	0.03	4.74	1.18	2.30	—
32-2, 16–18	1.13	0.91	3.73	−0.07	3.38	1.19	2.30	—
32-3, 22–24	0.46	0.76	4.57	0.10	4.43	0.91	2.18	—
33-1, 80–82	1.31	0.79	3.62	0.08	3.80	1.10	2.26	—
33-2, 101–103	—	0.79	2.56	−0.11	3.60	1.13	2.31	—
33-3, 118–120	—	0.83	3.82	0.33	4.00	1.14	2.31	—
34-1	—	1.65	7.54	2.23	8.07	1.05	2.26	—
34-2	—	0.90	7.20	1.09	5.27	1.05	2.31	—
35-1	—	0.77	3.84	0.29	3.37	1.01	2.26	—
35-2	—	0.69	2.55	0.82	6.29	1.11	2.26	—
36-1	—	2.11	10.49	4.35	12.41	0.98	2.03	—
36-2	—	3.66	18.00	8.57	19.88	0.95	2.26	—
Hole 521								
1-1, 19–21	2.67	2.08	6.55	1.27	8.49	1.52	—	2.10
1-1, 99–101	2.96	1.03	2.82	—	—	—	—	1.39
1-2, 109–111	1.58	0.40	1.29	—	—	—	—	1.92
2-1, 69–71	1.33	2.03	1.13	—	—	—	—	1.79
2-1, 82–84	—	0.65	2.43	—	—	—	—	1.76
9-1, 130–132	5.80	0.71	2.38	—	—	—	—	1.57
11-1, 38–40	—	0.67	2.57	−0.12	2.74	1.16	—	1.53
11-1, 48–50	—	0.68	3.00	0.73	2.74	1.28	—	1.62
11-1, 125–127	1.19	6.52	34.30	—	—	—	—	1.59
11-1, 135–137	—	7.12	36.90	5.17	33.40	0.99	—	1.45
16-1, 39–41	—	11.68	40.80	14.30	35.40	1.04	—	1.42
Hole 522								
1-1, 24–26	8.48	2.21	2.10	—	7.30	1.61	—	2.13
1-1, 144–146	14.71	3.21	11.29	—	—	—	—	2.29
1-2, 101–103	1.83	0.41	0.92	—	—	—	—	2.13
2-1, 102–104	1.58	0.55	1.94	—	—	—	—	1.77
2-2, 50–52	0.58	0.77	2.33	—	—	—	—	1.70
6-1, 101–103	0.72	0.44	1.10	—	2.90	1.48	—	1.80
10-3, 30–32	9.54	7.80	39.75	—	35.82	1.04	—	1.55
16-1, 144–146	2.26	—	—	—	10.84	1.04	—	1.42
35-1, 84–86	1.21	1.05	4.37	—	2.40	0.98	—	1.51

[a] Exact position of some sediment samples is unknown.

Table 1B. Downhole variation of the magnetic hysteresis and the magnetic remanence parameters for Hole 523.

Core-Section (interval in cm)	NRM (10^{-6} Am^2/kg)	M_{rs} (10^{-3} Am^2/kg)	χ_i (10^{-8})	χ_h (10^{-8} m^3/kg)	M_s (10^{-3} Am^2/kg)	H_c (10^4 A/m)	H_{cr} (10^4 A/m)	MDF (10^4 A/m)	Color
6-2, 64-66	0.97	1.43	6.22	1.21	6.68	1.25	2.48	2.13	Light brown
6-3, 64-66	0.77	0.75	3.40	—	—	—	—	2.18	Very light brown
7-1, 114-116	0.68	0.43	1.26	−0.40	1.67	1.43	2.86	2.22	White
7-3, 10-12	0.27	0.57	2.36	—	2.19	1.09	2.23	1.45	White
10-1, 120-122	6.65	6.21	30.43	11.60	46.50	1.02	2.40	1.70	Dark red
10-2, 90-92	8.77	7.29	33.36	10.60	49.30	1.67	2.46	1.60	Dark red
10-3, 50-52	4.73	8.44	32.83	10.50	73.63	1.01	1.98	1.42	Dark red
12-2, 23-25	1.07	2.16	8.86	1.15	11.00	1.07	2.12	1.45	Light brown
16-1, 74-76	0.84	2.39	12.53	—	—	—	1.96	1.70	Medium brown
16-1, 114-116	2.93	2.37	11.10	—	—	—	1.78	1.35	Brown and white
17-1, 42-44	1.49	1.04	4.59	—	—	—	1.91	1.53	Brown and white
19-1, 90-92	1.62	3.31	16.62	3.62	17.61	1.04	1.87	1.72	Dark brown
19-2, 54-56	2.39	1.24	5.78	—	—	—	2.05	1.87	Light brown
26-1, 70-72	2.35	0.63	2.36	−0.43	—	—	2.00	1.59	White
27-1, 122-124	2.75	0.55	1.95	—	—	—	2.02	1.57	White
28-1, 123-125	3.72	2.18	9.68	—	10.31	1.09	2.01	1.65	Medium brown
28-3, 87-89	9.11	3.03	16.03	—	—	—	2.02	1.66	Medium brown
30-1, 129-131	6.89	1.85	9.00	—	9.93	0.98	2.00	1.50	Medium brown
32-2, 54-56	0.63	3.81	16.70	2.18	22.63	1.05	1.83	1.45	Dark brown
33-2, 84-86	1.61	1.57	10.35	—	—	—	1.95	1.55	Light brown
35-2, 10-12	1.98	5.07	36.90	1.70	50.77	0.88	1.89	1.46	Dark brown and white
37-2, 105-107	6.03	1.79	8.49	0.63	12.41	0.99	1.88	1.44	Medium brown
38-2, 34-36	2.43	1.98	9.23	—	—	—	1.72	1.37	Dark brown and white
39-1, 64-66	2.84	3.96	23.40	3.06	13.26	0.96	1.72	1.41	Medium brown
42-1, 114-116	4.17	1.66	8.40	0.65	9.31	0.99	2.11	1.37	Yellow brown
42-3, 79-81	3.17	1.66	9.27	—	—	—	2.11	1.26	Yellow brown
44-2, 50-52	2.78	1.75	9.27	0.31	12.45	0.96	1.75	1.44	Yellow brown
45-2, 100-102	1.27	1.69	8.75	0.93	7.12	0.84	1.71	1.41	Yellow brown
48-1, 99-101	1.03	1.44	7.44	1.34	9.80	0.97	2.00	1.24	Medium brown
49-2, 105-107	0.77	1.00	4.29	0.62	6.48	0.97	2.07	1.53	Yellow brown
50-1, 123-125	0.99	1.32	7.14	0.77	9.20	1.08	1.79	1.73	Light brown
50-2, 40-42	3.56	1.56	7.08	0.98	9.81	0.87	1.84	1.42	Yellow brown

Table 1C. Downhole variation of the magnetic hysteresis and the magnetic remanence parameters for Hole 524.

Core-Section (interval in cm)	NRM (10^{-6} Am^2/kg)	M_{rs} (10^{-3} Am^2/kg)	χ_i (10^{-8})	M_s (10^{-3} Am^2/kg)	H_c (10^4 A/m)	H_{cr} (10^4 A/m)	MDF (10^4 A/m)	Grain size
9-1, 143-145	21.75	3.49	14.49	—	—	2.75	1.33	Fine
10-5, 98-100	2.35	2.45	9.95	—	—	2.61	1.32	Fine
11-3, 61-63	11.62	5.09	20.41	31.03	1.08	2.50	1.40	Fine
11-3, 66-68	4.42	5.34	20.84	33.69	1.08	2.55	1.37	Medium
11-3, 71-73	0.71	3.36	14.29	21.69	1.09	2.61	1.56	Coarse
11-3, 76-78	0.84	4.08	18.08	24.27	1.08	2.56	1.66	Coarse
11-3, 81-83	11.19	7.06	16.65	38.47	1.06	2.36	1.31	Fine
11-3, 92-94	11.81	8.71	38.34	60.99	1.08	2.37	1.30	Fine
12-4, 9-11	10.38	6.70	32.09	—	—	2.29	1.34	Fine
12-4, 12-14	1.43	5.14	23.49	—	—	2.37	1.30	Coarse
12-4, 15-17	1.89	9.30	41.48	—	—	2.52	1.28	Coarse
12-4, 20-22	10.46	8.92	45.30	—	—	2.27	1.27	Fine
13-5, 31-33	9.27	10.91	38.60	—	—	2.33	1.14	Fine
14-2, 127-129	3.21	4.50	16.51	—	—	2.54	1.56	Fine
17-4, 55-57	23.39	—	—	92.14	1.20	—	—	Fine
19-3, 56-58	14.00	—	—	88.32	1.04	—	—	Fine
21-2, 21-23	142.54	26.66	144.36	—	—	2.16	1.17	Fine
22-4, 114-116	11.38	21.65	73.81	—	—	2.40	1.33	Coarse
22-4, 119-121	29.45	22.95	109.14	—	—	2.46	1.29	Fine

The main trends in behavior are clear. First, the lightest sediments produce loops that are small in vertical scale (i.e., low M_s) and have negative high-field slopes (χ_h). Second, with a darkening in color, M_s increases and χ_h becomes increasingly positive. And third, the width of the loops is marginally smaller for the darker than for the lighter-colored sediments nearby. Relatively narrow loops are an indication of low magnetic stability. This will be discussed further below. The magnitudes of M_s and χ_h depend on both the concentration and the composition of the constituent magnetic minerals. As will be shown later, the primary magnetic minerals are near magnetite in composition. By taking the value of M_s for pure magnetite (95 Am^2/kg), we can derive the approximate concentration of the magnetic mineral fraction of the sediment. At Site 519, M_s varied between 1.3×10^{-3} and 20×10^{-3} Am^2/kg, indicating that the stable magnetic fraction may comprise as little as 15 to 200 ppm of the whole sediment.

The relationship between color, carbonate content, and the bulk hysteresis properties are shown in Figures 1 and 3. The values of χ_h that have been plotted are corrected to take account of the diamagnetism of the sample holder and the estimated diamagnetic contribution from the carbonate. The residual χ_h values give an approximate contribution for the paramagnetic minerals plus a contribution from any residual diamagnetic minerals. In view of the uncertainties in applying this correction, an error of up to 5×10^{-9} m^3/kg is estimated for the results. Although the $CaCO_3$ analyses were per-

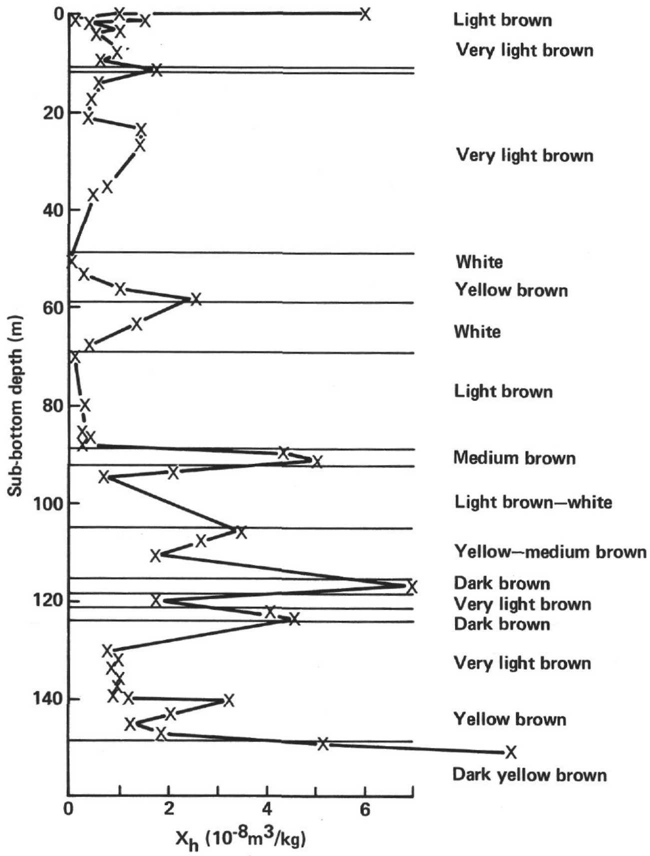

Figure 3. Downhole variation of susceptibility (Hole 519).

formed on a different subset of samples, there does seem to be a positive correlation between noncarbonate content and both M_s and χ_h. The ratio M_s/(percent noncarbonate) does not vary systematically with either color or depth, and the ratio of highest to lowest values within each individual set of measurements comes out at around the value 8 in both cases. Similarly, the ratio χ_h/(percent noncarbonate) seems to be largely independent of the carbonate content, although within error limits there may be a peak in this ratio at the lower carbonate concentrations.

The above results point strongly toward a concentration effect, the carbonate acting to dilute the magnetic fraction. It follows that no gross change in the magnetic mineralogy of the stable magnetic fraction was associated with the concentration. This implies that the magnetic detritus may have always formed roughly the same fraction of the noncarbonate input and that it never fluctuated significantly in composition. With any subsequent dissolution of the carbonate (i.e., volume reduction), the stably magnetized grains remained largely unaffected, being concentrated without any gross chemical alteration. The concentration of a pre-existing high-coercivity and/or paramagnetic phase is also consistent with this hypothesis. However, as a result of the limitations on the accuracy of experimental measurement, it remains unproven whether such material existed in the very dilute detritus. At least some of these magnetic components may have grown authigenically under the conditions that existed during the dissolution event.

The concentration hypothesis can be tested by comparing the accumulation rate curves deduced from the magnetostratigraphy to the inverse of M_s. Figure 4 shows a good correlation, or at least no significant discrepancies, after allowing for the higher resolution in the rates deduced from M_s. The correlation does of course break down around 15 to 30 sub-bottom, where the inclusions of slumped material were present. The similarity in shape of the remainder of the curves supports the concentration hypothesis. Although the evidence is by no means conclusive, we feel that the curve derived from the NRM may be displaced downward with respect to that derived from M_s. If this is correct, then it would imply a significant lag in the blocking of the

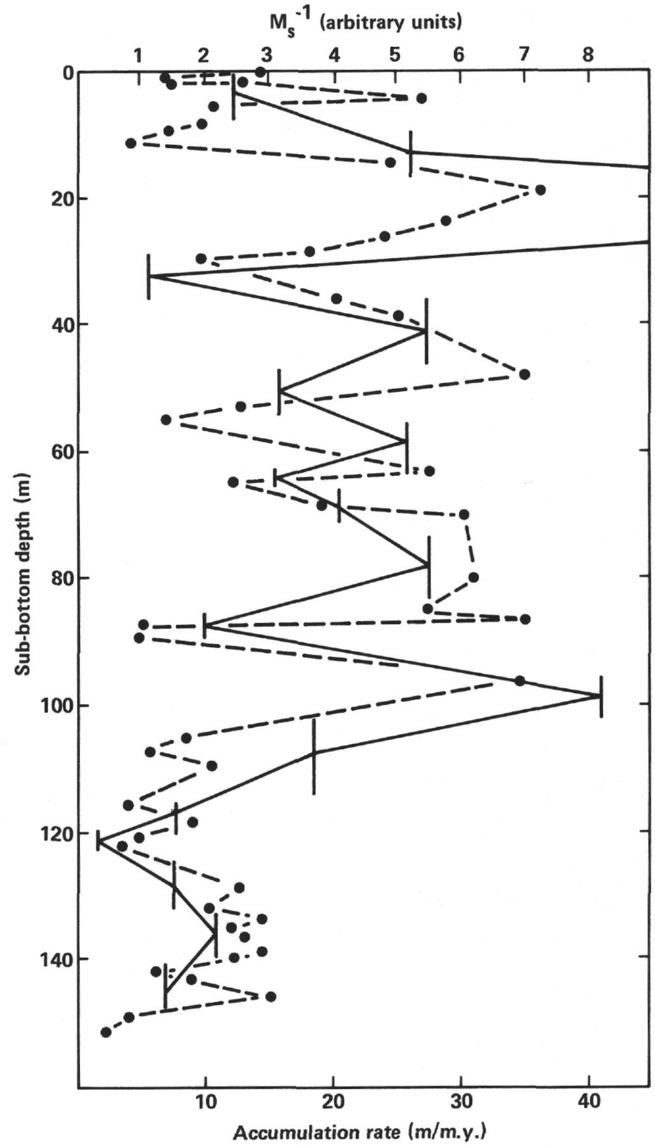

Figure 4. Comparison of the sedimentation rate curves derived from the magnetostratigraphy (solid line) and from the saturation magnetization (dotted line). Hole 519.

NRM with respect to the initial deposition and would provide strong evidence for postdepositional realignment as the dominant recording mechanism. With a higher sampling density, the above technique has the potential to (1) refine the high-resolution accumulation rate curves that are available from the magnetostratigraphy of piston-core sediments, (2) monitor any gross changes in magnetic mineralogy, and (3) define the depth at which the NRM is blocked in.

Magnetic Stability and Domain State

The coercive force, H_c (which is equivalent to half the central width of the hysteresis loop), is shown as a function of depth and color in Figure 5. It is clear that the variations in color only impose local fluctuations on the overall trend from high to low coercivities down the core. Other measurements of stability include the median destructive field (MDF) of a saturation isothermal remanence (M_{rs}) and the remanent coercivity, H_{cr} (Table 1 and Fig. 5). All these parameters show the same downhole trend as H_c. A dark sediment is always of lower stability than an adjacent lighter-colored sediment. However a young dark sediment is not necessarily of lower magnetic stability than a much older but lighter sediment (Fig. 6). For example, a white sediment in Sample 523-27-1, 122–124 cm, which is 37 m.y. in age, has a significantly lower coercivity of remanence than a dark brown sediment (Sample 519-29-2, 58–60 cm) 6 m.y. in age.

Coupled with the fall in magnetic stability with increasing depth are a rise in effective mean grain size,

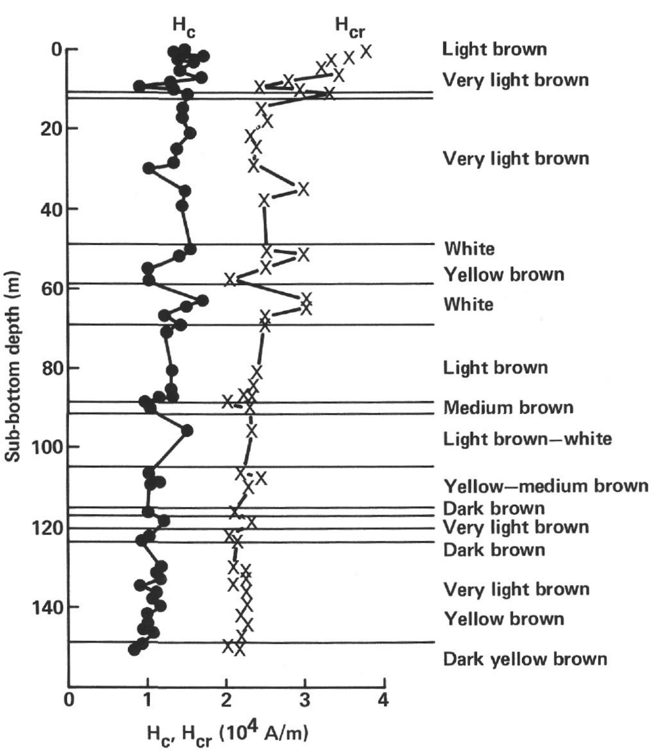

Figure 5. The downhole variation of the coercive force (H_c) and the coercivity of remanence (H_{cr}). Hole 519.

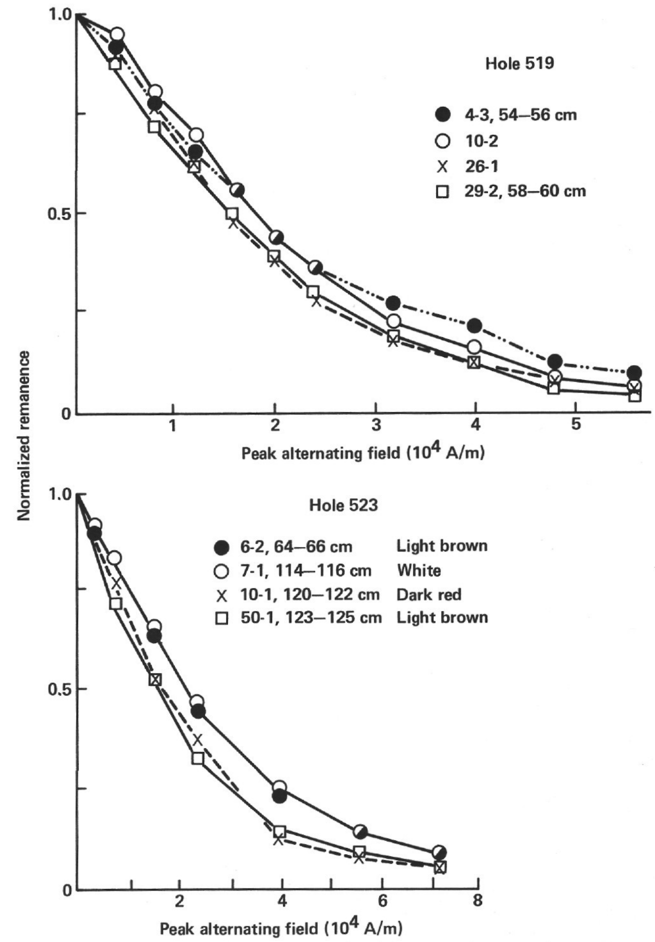

Figure 6. Alternating field demagnetization curves for selected sedimentary samples showing the variations with depth of burial and color.

shown by the increase in the H_{cr}/H_c ratio, and a trend toward a greater fraction of multidomain grains, as shown by a lowering of the M_{rs}/M_s ratio (Fig. 7). A more detailed discussion of the significance of these parameters can be found in, for example, Day et al. (1976). Although interpretation has largely been on the basis of magnetic grain size, it should be noted that magnetic interactions between adjacent grains can lower M_{rs}/M_s, as can inclusions of minerals carrying a viscous remanent magnetization (VRM).

In summary, the changes mentioned above can be brought about by a shift in the magnetic grain-size distribution toward larger sizes, a chemical genesis of a relatively low-stability magnetic phase, or by physical concentration perhaps enhanced by a clustering of the magnetic grains.

BULK MAGNETIC HYSTERESIS PROPERTIES AS A FUNCTION OF AGE

There was no overall downhole trend in the saturation magnetization and high-field susceptibility for Holes 519 and 523. Further, sediments from similar lithologies from these two sites gave similar results. That is, a white sediment returned consistent values for M_s and χ_h ir-

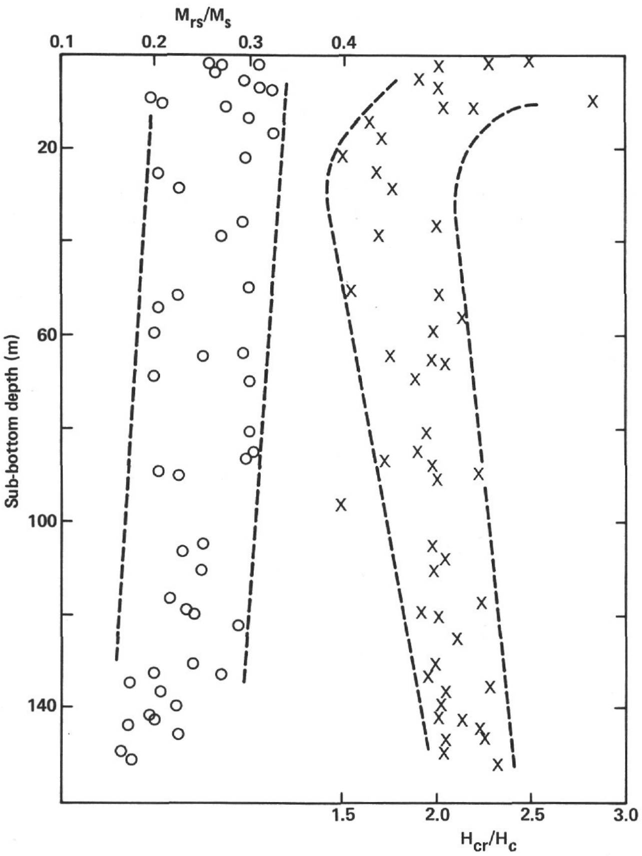

Figure 7. The downhole trend of the ratios M_{rs}/M_s and H_{cr}/H_c indicative of the domain state and mean magnetic grain size, respectively. The envelopes show the general trend in results.

respective of its time of formation or geographical location.

The magnetic stability parameters did, however, show a trend toward lower values with depth of burial (Figs. 5, 6, Table 1). More significantly, when the stability characteristics are replotted as a function of age rather than depth and the results from all holes are compared (Fig. 8), the trend in values remains. The magnitude of the coercivity parameters and their rate of change is, within experimental limits, identical for sediments of a similar age but taken from a wide geographical area.

A progressive decrease in H_c, H_{cr}, and MDF occurs during the first 10 m.y. after burial. For sediments older than 10 m.y., any further decrease in stability is slight. The downhole trends in H_c and H_{cr} are at a high level of statistical significance (Spearman's rank correlation coefficient, $\varrho = -0.76$ and -0.73, respectively). The M_{rs}/M_s ratio also decreases with age, although at a level below significance ($\varrho = -0.46$). H_{cr}/H_c, however, decreases for the first million years (down to a depth around 5 m in Hole 519); it then shows a steady rise and reaches a limiting value at around 10 Ma. The presence of the minimum may indicate a divide between a near-surface regime (Type 1) and one that is dominated by age, totally independent of depth of burial (Type 2). It should be remembered that superimposed on these behavioral regimes are the color fluctuations in stability,

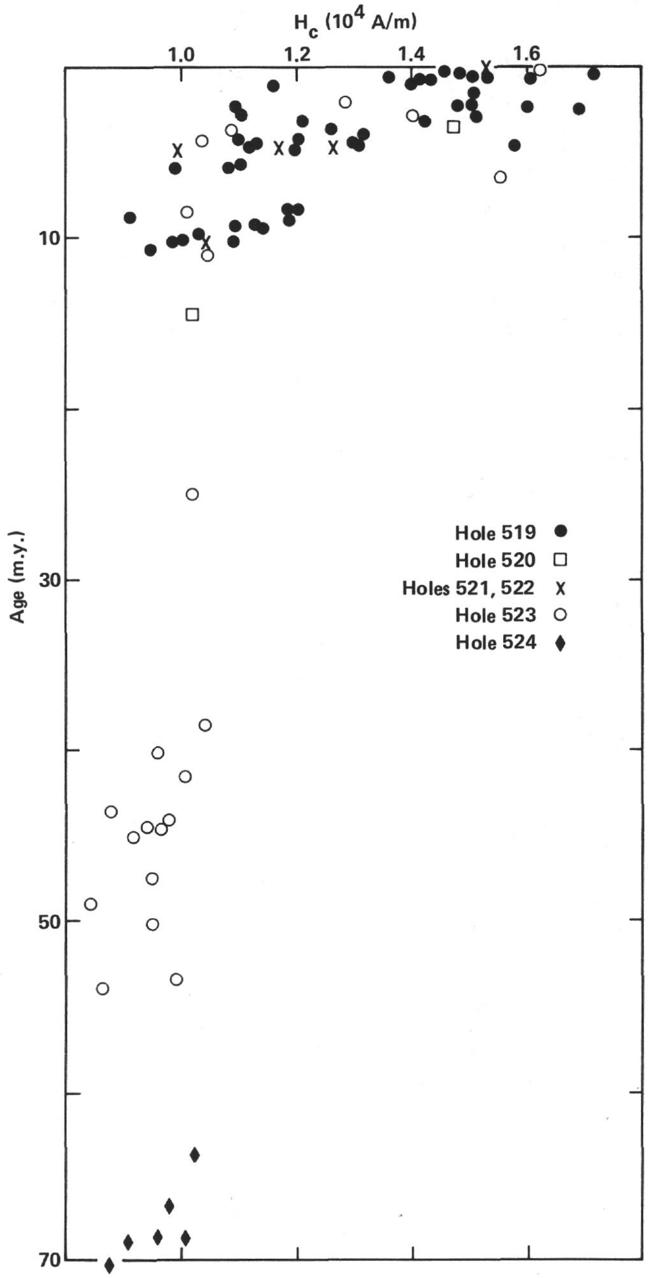

Figure 8. The variation in coercive force as a function of age of the sediment.

which may well be due to a third independent mechanism (Type 3).

OTHER MAGNETIC MEASUREMENTS

The variation of intensity of a saturation isothermal remanence, originally given at room temperature, was monitored while the sample was cooled in zero field down to 77°K (−196°C). The measurements were performed on partially dried samples to preclude the possibility of grain disturbance from the freezing of the interstitial water (Stober and Thompson, 1977). There is a possibility, however, that this treatment caused a slight degree of alteration. The cooling curves are shown in

Figure 9. Little change in remanence was seen for the topmost sediments. At a depth of 14 m a broad minimum, at around −80°C, became apparent. From 14 m to 29 m this drop in remanent intensity appeared to increase in magnitude, move toward higher temperatures, and become sharper. Below 29 m the magnitude of the drop decreased, although the trend toward higher temperatures with increasing depth remained.

Sharp changes in remanence on cooling have been associated with magnetic transitions. The Morin transition of hematite is around −15°C. A remanence minimum corresponding to a minimum in anisotropy is observed with the titanomagnetite solid solution series (Syono, 1965). The position of the remanence minimum denotes composition; its height is a complex function that depends on the fraction of multidomain material, the geometrical configuration of the remanence carriers, and the dominant anisotropy (e.g. Tucker, 1981). A remanence change could also indicate the blocking of a superparamagnetic fraction or of a low Curie point phase.

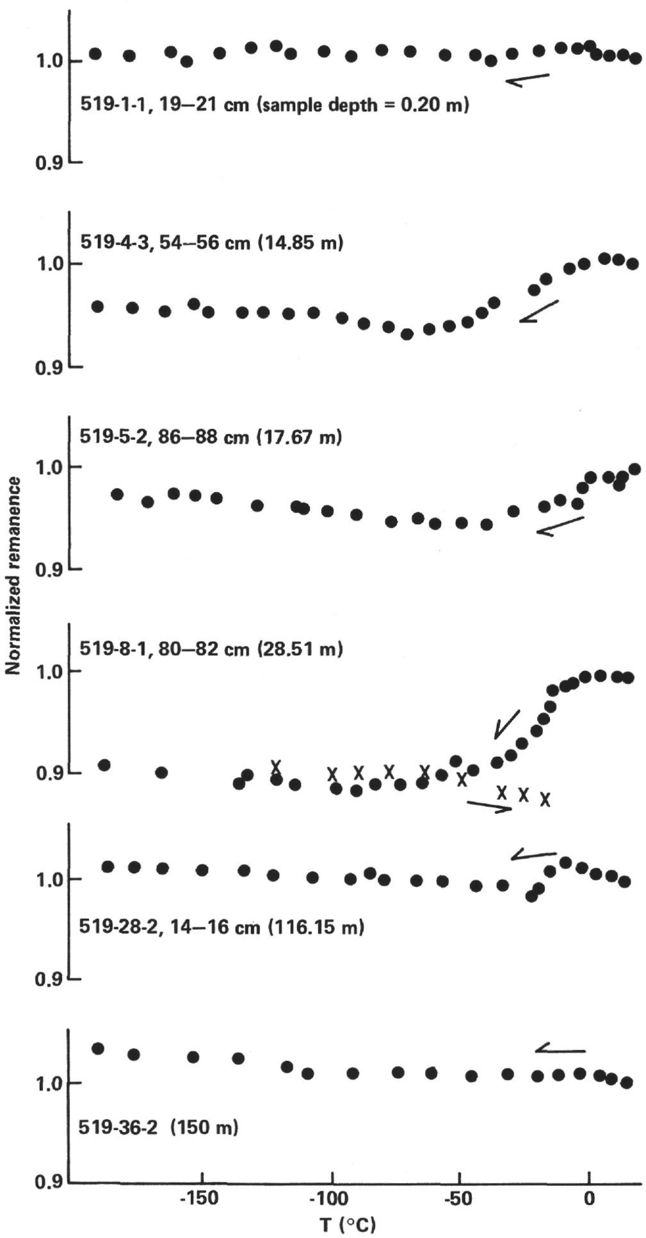

Figure 9. Cooling in zero field of the saturation isothermal remanent magnetization for selected samples from Hole 519. Arrows show direction of temperature change; symbol shapes distinguish cooling from rewarming data.

The results from Figure 9 indicate that there may be a change in magnetic mineralogy with depth. One possible interpretation is that a secondary spinel phase evolves and becomes progressively more enriched in titanium with time. It could be the daughter product from a chemical alteration or unmixing of the primary magnetic phase. Alternatively, the step in remanence just below 0°C may just be an indication of a fairly pure but not ultrafine hematite (Dunlop, 1971); a third possibility is that secondary hemoilmenite, near to ilmenite in composition, has been produced. The significance of a Morin transition in the white sediments (Cores 4 and 5) would be that the presence of hematite is established in the carbonate-rich sediments (i.e., prior to concentration through dissolution).

A transition at −10 to −15°C is also apparent for the dark red clays (Tucker, this vol.) but, surprisingly, not for the dark brown sediments from Hole 519, Core 36. The magnetic stability of Core 36 was high relative to the sediments immediately above (Tauxe et al., this vol.) and is thought to be the result of the diffusion of iron-bearing minerals from the bedrock as well as the concentration or diagenesis of the original magnetic carriers.

The absence of a transition at around 118°K for all sediments investigated (except for the volcaniclastic sands and clays of Hole 524) does not preclude the presence of magnetite. If magnetite is present it must be in the form of elongated or strained monodomain grains. Alternatively, the results could point to a "magnetite" containing between 10 and 40% ulvite in solution as the major magnetic mineral.

Residual material left over from the paleomagnetic sampling was reconstituted, samples being lumped together over coarse depth intervals. A magnetic extract was obtained from each bulk sample. The high-temperature variation of the initial susceptibility (χ_i) was measured for the extracts. A sharp drop in χ_i is associated with heating through the Curie temperature (T_c) of the magnetic constituent. Selected χ_i versus T curves are shown in Figure 10. The inferred values of T_c (all around 580°C) are indicative of magnetite. A low instrumental signal/noise ratio, necessarily incurred with small samples derived from a very limited quantity of source material, precluded any search for secondary magnetic phases. It is noted, however, that the fall in χ_i near to T_c became progressively less sharp for the older sediments.

X-RAY FLUORESCENCE MEASUREMENTS

The concentrations of iron, manganese, and titanium were measured for discrete samples from Site 519 by X-

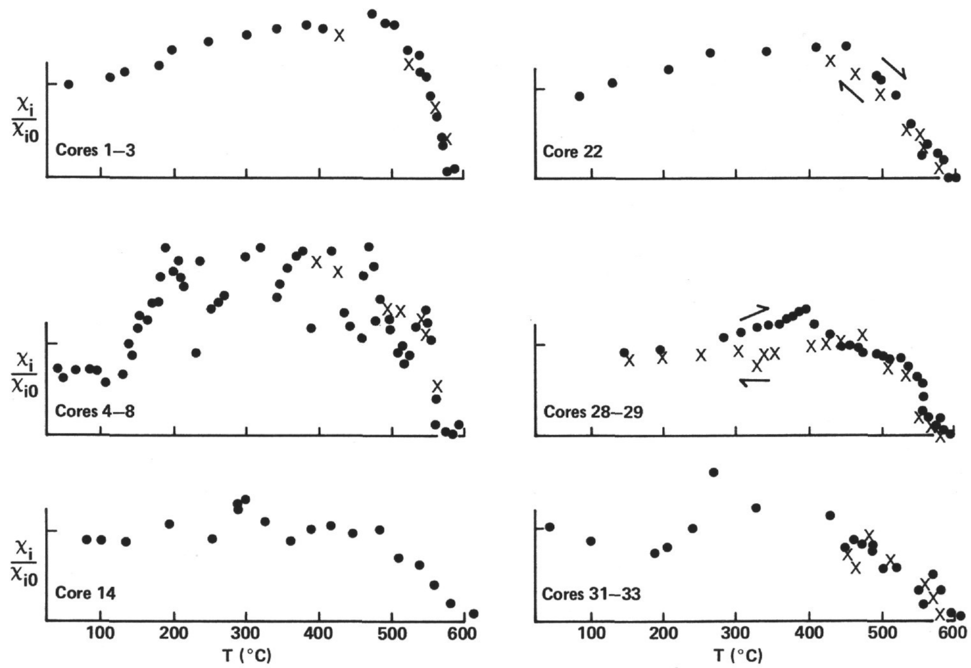

Figure 10. Initial susceptibility versus temperature curves for composite samples from Hole 519. Arrows and symbols as defined in Fig. 9. χ_{io} = initial susceptibility at room temperature.

ray fluorescence (XRF) analysis. The absolute concentrations of each element and the precise concentration ratios are not accurately defined as yet. The results are given (Fig. 11) in terms of relative concentration ratios reflecting the relative changes of Mn and Ti with respect to Fe down the cores.

The proportion of manganese to iron does not show any systematic trend with either depth or color. The titanium/iron ratio, however, increases by a factor of 2 down through the uppermost 10 m of sediment and then remains roughly constant for greater depths. There is no obvious connection between the Ti/Fe ratio and color. The relative change in Fe concentration alone as a function of color is consistent with the corresponding relative change in M_s.

The above evidence supports the hypothesis that it is the concentration of the noncarbonate fraction through dissolution rather than the precipitation of authigenic minerals from the bottom waters that leads to an enhancement of the stable and unstable components of remanence. It must be remembered, however, that the XRF results were obtained on the whole sediment and not just on the magnetic fraction. We do not know whether changes in the elemental abundances in the bulk sediment truly represent any changes in the magnetic fraction alone. Conceivably, on concentration, there may be a rearrangement of the localized elemental distribution. For example, Cores 28, 29, 35, and 36 of Hole 519 contain an abundance of manganese micronodules, whereas Cores 30 to 34 contain very few (Karpoff, this vol.). The elemental Mn/Fe ratio does not show any corresponding variation. Preliminary qualitative microprobe analysis has failed to find any concentration of iron above the background level to be associated with the manganese-rich regions within the sediment. There is no strong correlation between the bulk manganese concentration (both for the dispersed state and for concretions) and the bulk stability. The coercivities for Cores 28, 29, 35, and 36, where manganese micronodules are plentiful, are only marginally lower than those for Cores 30 to 34, where there are very many fewer. It is the dependence on depth, independent of manganese concentration, that dominates the variation in bulk coercivity. We conclude that the intrinsic magnetic character of the South Atlantic sediments is only very weakly influenced, if at all, by the relative abundance of manganese-rich minerals.

The lack of trend in the Ti/Fe ratio below 20 m shows that no preferential dissolution or precipitation of these two elements is closely associated with the magnetic fraction of the sediment. Near the surface, the titanium content built up or the iron content became progressively more depleted with depth (or age). If this is indicative of a change in the magnetic grains, there should be a change in the magnetic properties themselves. In particular the possible evolution of a titanium-rich phase (titanomagnetite or hemoilmenite) could account for the onset of the remanence steps (on cooling) at depths of a few meters into the sediment. It may also explain the blurring of the Curie temperatures as the result of chemical alteration of the original magnetic phase. The end result of this alteration must account for the decrease in coercivity and the fall in the H_{cr}/H_c ratio. The kinetics of alteration would be more rapid for the smaller grains, with their high specific surface area. Thus, there could be a reduction in the effective proportion of fine to coarse grains. A change in overall grain anisotropy may also be associated with the alteration, which acts in the sense leading to lower coercivities. We do not as yet have sufficient data to define the exact

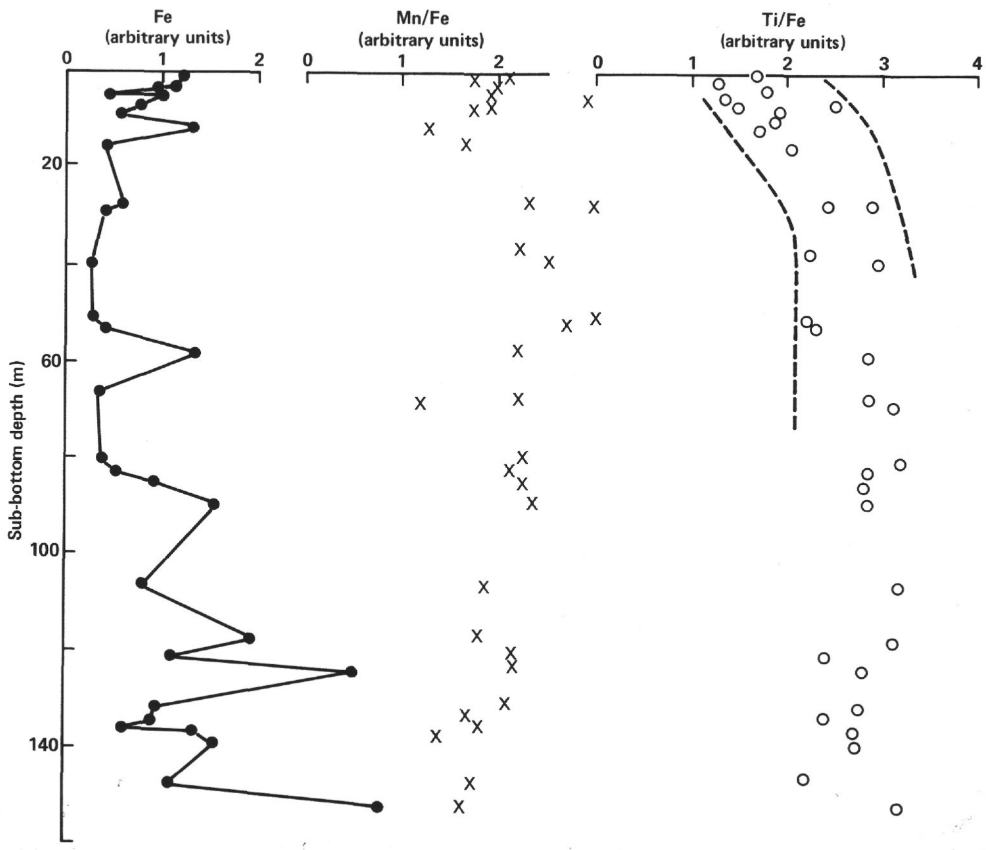

Figure 11. The relative changes in the abundance of iron and the relative proportions of manganese to iron and titanium to iron, plotted as a function of depth. Hole 519.

nature of dominant grain anisotropies. Both of the above mechanisms are discussed by Day et al. (1976).

NATURAL REMANENT MAGNETIZATION

A decrease in NRM stability with depth was observed for the Leg 73 sediments. In particular, at Site 519, a stable magnetization direction for the uppermost sediments was achieved after AF demagnetization to peak fields of less that 8×10^3 A/m, whereas for the deeper sediments, demagnetization fields of 12×10^3 A/m were necessary before a stable direction was reached. The darker sediments generally required a higher cleaning field than those lighter in color. The intensity of the viscous part of the remanent magnetization also showed a strong positive correlation with the darkness of the sediment (Table 2).

Statistical analysis of the magnetization directions averaged over each core length (Hole 519) showed a progressive increase in scatter (i.e., increase in α_{95}) with depth of burial (Fig. 12). Cores containing mainly dark sediments showed, in general, more scatter in the stable directions than adjacent cores composed mainly of lighter material.

The magnitude of the NRM often decreased with depth (Tauxe et al., this vol.). This effect was most pronounced immediately below the sediment surface. The ratio NRM/M_{rs} describes the observed remanence as a fraction of the maximum possible remanence. It should correct for variations in concentration of the source material. For samples from Holes 519, 521, and 522 there was a marked decrease in NRM/M_{rs} through the uppermost few meters (Fig. 13). Any further systematic decrease at greater depths was small. Localized decreases in NRM/M_{rs} were associated with the more disturbed sediments, however (Tucker, this vol.). The interpreta-

Table 2. The viscous remanent magnetization acquired in a laboratory field of 21 A/m (0.27 Oe) over a period of 2 weeks. Samples are from Hole 519.

Core-Section (interval in cm)	Stable NRM (10^{-6} Am^2/kg)	VRM (10^{-6} Am^2/kg)	VRM / Stable NRM (%)
1-1, 79-81	7.71	2.80	39
1-2, 24-26	4.09	0.21	5
1-2, 44-46	1.54	0.05	3
2-2, 115-117	20.73	0.37	2
4-3, 33-35	1.41	0.16	11
4-3, 100-102	3.48	0.01	0
7-1, 120-122	1.09	0	0
10-1, 32-34	3.12	0.60	19
10-1, 90-92	2.33	0.04	2
13-2, 30-32	18.07	1.25	7
13-2, 60-62	1.11	0.35	31
17-1, 92-94	1.00	0.07	6
21-2, 60-62	1.35	0.19	14
21-3	0.37	0	0
23-1	0.29	0.06	20
26-2	1.31	0.17	13
28-2	2.01	0.92	46
29-1	0.71	1.30	183
29-3	0.74	0.31	42
29-3	1.32	0.91	69

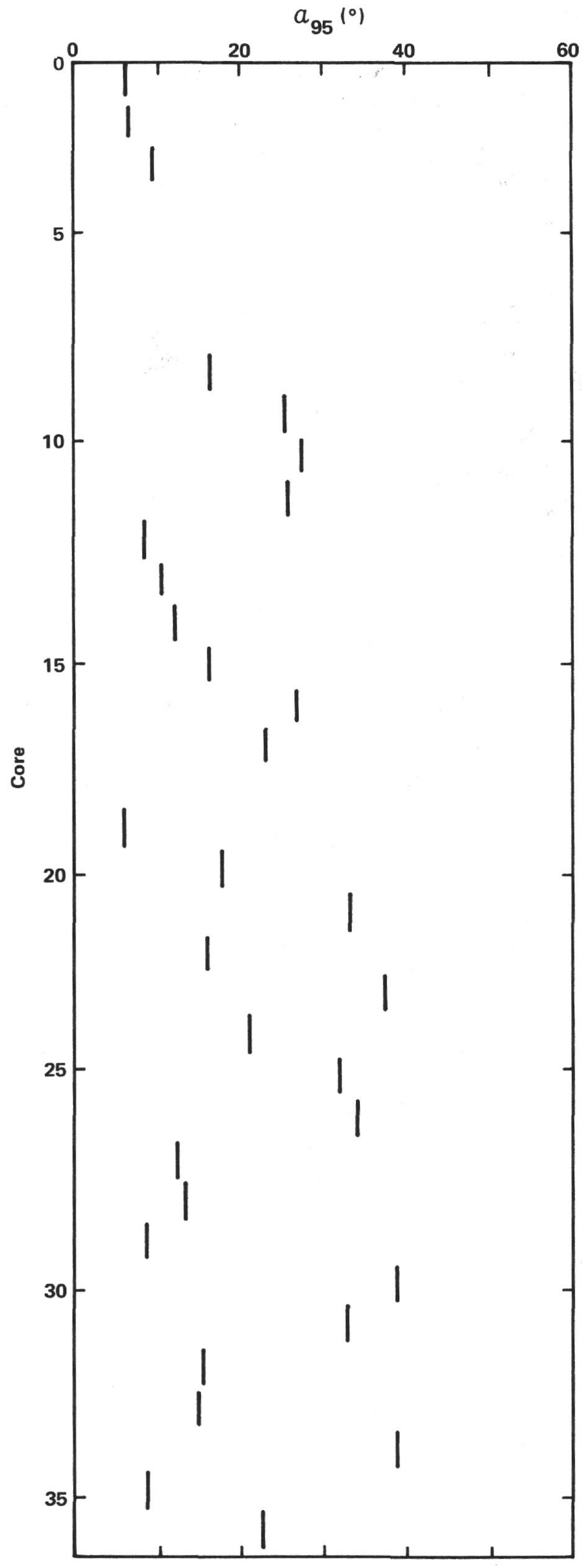

Figure 12. The variation with depth of the 95% confidence limit on the mean stable remanence direction for each core length. Hole 519. The α_{95} values were derived from Fisher statistics on the paleomagnetic directions (the reversed polarities rotated through 180°). High values of α_{95} are indicative of a large amount of scatter between results.

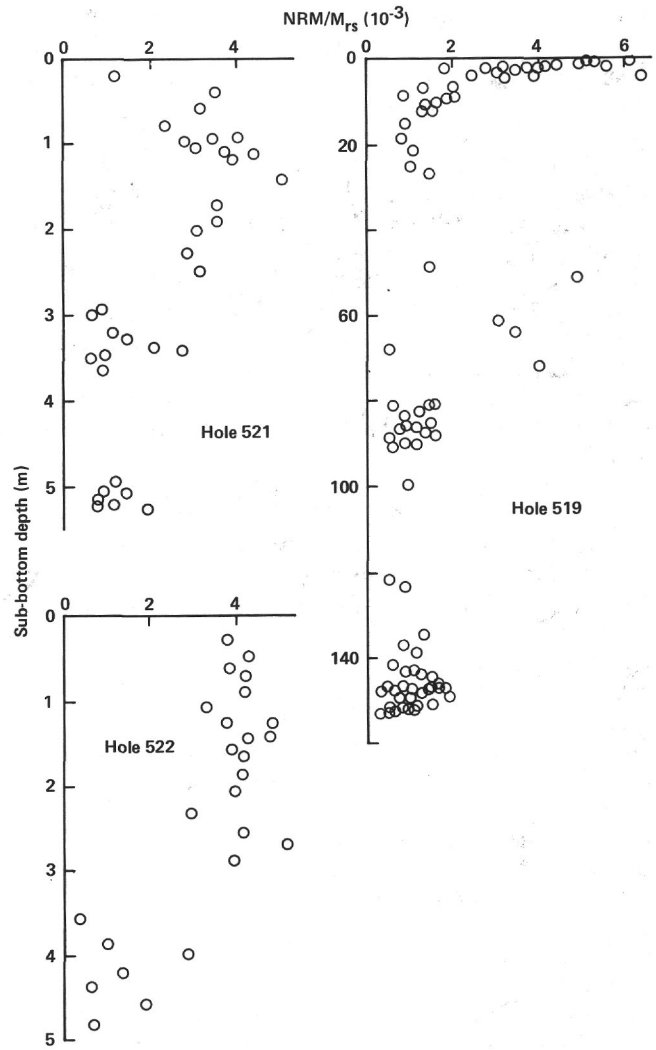

Figure 13. The normalized NRM intensity for near-surface sediments from Holes 519, 521, and 522.

tion of NRM intensities is complicated by the dependence of NRM on many variables. The intensity depends not only on the applied field strength but also on the physical structure of the sediment and on the physical and chemical state of the magnetic grains. Further, the record is not an instantaneous reading of the ambient field vector but rather a time average. This in turn may lead to the recording of very low intensities near a polarity transition (Løvlie, 1976). The changes in normalized NRM intensity (Fig. 13) may thus be related to the change in the field polarity at the onset of the Bruhnes Epoch (0.7 Ma). Thereafter, conceivably, the deeper sediments may have been partially remagnetized (i.e., acquired a PDRM, VRM of CRM) in the present-day field. The possibility that the intensity of the Earth's field was significantly higher during the Brunhes than at any time previously remains very unlikely. A physical randomization of the grains through, for instance, compaction could produce the observed intensity shift. We feel that the most likely interpretation, however, is that a progressive chemical alteration of the magnetic grains occurs at and just below the sediment surface. The longer-term decreases in NRM stability occur with, at most, a very small corresponding decrease in NRM/M_{rs}. It may well be that these two types of behavior are linked with the bulk stability of the sediment (Types 1 and 2, as discussed earlier).

A preferential dissolution or alteration of the smaller grains has been proposed to account for the observed stability decrease with depth. The grains affected are usually the prime carriers of the original NRM. A reduction in their number would obviously lead to a fall in NRM intensity. A reduction in their effective size from single domain to superparamagnetic would also reduce the stable remanence and perhaps introduce an unstable or viscous component of magnetization. Alteration into a more weakly magnetized phase could produce a similar effect.

SUMMARY AND CONCLUSIONS

We have discussed the results and possible causes controlling the magnetic characteristics of the sediments from Leg 73, both as a function of depth (age) and color. We have tentatively divided the observed variations into three regimes: (1) near surface (or 0–1 Ma), (2) 1 to 10 Ma, and (3) with increasing dissolution. The bulk magnetic properties, the NRM and other remanence characteristics, and the relative elemental abundances can all be fitted into the above scheme. A summary is given in Table 3. Although as yet we have insufficient data to form definite conclusions on the various mechanisms of alteration, we will present our working hypotheses bases on our current understanding.

Type 1

We attribute the near-surface effects to be the result of progressive oxidation in the oxygen-rich bottom waters. On the basis of the XRF results, we believe that oxidation proceeds through the preferential dissolution of iron from the magnetic spinel phases rather than the incorporation of extra oxygen into the lattice. The process produces a change in composition of the major magnetic carriers. The daughter products are enriched in titanium with respect to the source material. There may be a reduction in the effective proportion of stably magnetized fine grains. If this mechanism holds, it would imply that the leached iron is not re-precipitated nearby in the form of secondary minerals.

Table 3. Summary of the magnetic properties for sediments from Hole 519.

	Type 1	Type 2	Type 3
Region where active	Near surface (0–1 Ma)	1–10 Ma	Partially dissolved facies
Property	Variation with depth (age)	Variation with depth (age)	Variation with increasing dissolution
Induced magnetism	Independent	Independent	M_s, χ_i, χ_h increase
Bulk stability	H_c, H_{cr} decrease	H_c, H_{cr} decrease	H_c, H_{cr} decrease slightly
Magnetic grain size/ domain state	H_{cr}/H_c decreases, M_{rs}/M_s decreases	H_{cr}/H_c increases, M_{rs}/M_s decreases	H_{cr}/H_c increases slightly, M_{rs}/M_s decreases
NRM stability	Decreases	Decreases	Decreases
NRM intensity	NRM/M_{rs} decreases rapidly	NRM/M_{rs} decreases slightly	NRM/M_{rs} decreases
Elemental ratios	Ti/Fe increases, Mn/Fe remains constant	Independent	Independent

Type 2

This regime is more difficult to quantify. The oxidation process must have slowed down as the sediments became more isolated from the oxygen-rich bottom waters. Dissolution of the small grains may continue as the magnetic material equilibrates with its immediate environment.

Type 3

The results of the carbonate dissolution are primarily a concentration of the magnetic minerals. The elements associated with the magnetic character of the sediment do not vary in relative concentration. There is no evidence that the NRM is associated with manganese micronodules. We have not resolved whether the observed goethite is merely concentrated on dissolution or is produced by the chemical alteration of the iron-bearing minerals.

We believe that the decrease in NRM intensity and stability with age and, implicitly, the clarity of the paleomagnetic results are primarily the results of changes in the magnetic character of the grains themselves.

Previous rock-magnetic studies of pelagic sediments were largely confined to samples taken from the Pacific Ocean, where, of course, different mechanisms may prevail. Bearing this in mind, we conditionally support the oxidation theories (e.g., Johnson et al., 1975) and question the iron–manganese models (Henshaw and Merrill, 1980). We have given evidence in support of a new path for the oxidation, that is, through the preferential leaching of iron. Such a process has been proposed, and evidence for its occurrence in submarine basalts appears to be accumulating. Model mechanisms for the process have been discussed by O'Reilly (1981).

ACKNOWLEDGMENTS

We would like to thank Derek Albone for the XRF analyses and Bill O'Reilly for making available the facilities of the rock-magnetic laboratory at the University of Newcastle-upon-Tyne.

Dr. W. O'Reilly and Professor K. Creer kindly reviewed the manuscript. The work was financed by DSDP and NERC.

REFERENCES

Crecelius, E. A., Carpenter, R., and Merrill, R. T., 1973. Magnetism and magnetic reversals in ferromanganese nodules. *Earth Planet. Sci. Lett.*, 17:391–398.

Day, R., Fuller, M. D., and Schmidt, V. A., 1976. Magnetic hysteresis properties of synthetic titanomagnetites. *J. Geophys. Res.*, 81: 873–880.

Dunlop, D. J., 1971. Magnetic properties of fine-particle hematite. *Ann. Geophys.*, 27(3):269–291.

Haggerty, S., 1970. Magnetic minerals in pelagic sediments. *Ann. Rept. Geophys. Lab. Carnegie Inst.*, 68:332–336.

Henshaw, P. C., and Merrill, R. T., 1980. Magnetic and chemical changes in marine sediments. *Rev. Geophys. Space Phys.*, 18: 483–504.

Johnson, H. P., Kinoshita, H., and Merrill, R. T., 1975. Rock magnetism and paleomagnetism of some North Pacific deep-sea sediments. *Geol. Soc. Am. Bull.*, 86:412–420.

Kent, D. V., and Lowrie, W., 1974. Origin of magnetic instability in sediment cores from the central North Pacific. *J. Geophys. Res.*, 79:2987–3000.

Løvlie, R., 1976. The intensity pattern of post-depositional remanence acquired in some marine sediments during a reversal of the external magnetic field. *Earth Planet. Sci. Lett.*, 30:209–214.

Opdyke, N. D., Glass, B., Hays, J. D., and Foster, J. H., 1966. Paleomagnetic study of Antarctic deep-sea cores. *Science,* 154: 349–357.

O'Reilly, W., 1981. The identification of titanomaghemites. *Geophys. J. R. Astron. Soc.,* 65:271. (Abstract)

Powell, H. E., and Ballard, L. N., 1968. Magnetic susceptibility of 34 manganese bearing minerals. *U.S. Bur. Mines Inf. Cir.,* 8359:1.

Ryall, J. C., and Hall, J. M., 1979. Laboratory alteration of titanomagnetites in submarine pillow lavas. *Can. J. Earth Sci.,* 16(3), 496–504.

Stober, J. C., and Thompson, R., 1979. Magnetic remanence acquisition in Finnish lake sediments. *Geophys. J. R. Astron. Soc.,* 57: 729–739.

Syono, Y., 1965. Magnetocrystalline anisotropy and magnetostriction of Fe_3O_4–Fe_2TiO_4 series with special application to rock magnetism. *Jpn. J. Geophys.,* 4:71–143.

Tucker, P., 1980a. A grain mobility of post-depositional realignment. *Geophys. J. R. Astron. Soc.,* 63:149–163.

________, 1980b. Stirred remanent magnetization: A laboratory analogue of post-depositional realignment. *J. Geophys.,* 48:153–157.

________, 1981. Low-temperature magnetic hysteresis properties of multidomain single crystal titanomagnetite. *Earth Planet. Sci. Lett.,* 54:167–172.

Verosub, K. L., 1977. Depositional and post-depositional processes in the magnetization of sediments. *Rev. Geophys. Space Phys.,* 15(2): 129–142.

Date of Initial Receipt: November 30, 1981